

Climate change projections for olive yields in the Mediterranean Basin

Journal:	<i>International Journal of Climatology</i>
Manuscript ID	JOC-19-0237.R1
Wiley - Manuscript type:	Research Article
Date Submitted by the Author:	03-Jun-2019
Complete List of Authors:	<p>Fraga, Helder; Universidade de Trás-os-Montes e Alto Douro, Centre for the Research and Technology of Agro-Environmental and Biological Sciences</p> <p>Pinto, Joaquim; Karlsruher Institut für Technologie Institut für Meteorologie und Klimaforschung, Institute of Meteorology and Climate Research</p> <p>Viola, Francesco ; Università degli Studi di Cagliari, Department of Civil Environmental and Architectural Engineering</p> <p>Santos, João; Universidade de Trás-os-Montes e Alto Douro, Centre for the Research and Technology of Agro-Environmental and Biological Sciences</p>
Keywords:	Olive yields, climate change, Euro-Cordex, Representative Concentration Pathways, Europe, Climate < 2. Scale, Land-atmosphere < 4. Geophysical sphere, Agrometeorology < 6. Application/context
Country Keywords:	Spain, Portugal, France, Italy, Greece

SCHOLARONE™
Manuscripts

1 **Climate change projections for olive yields in the Mediterranean Basin**

2 Helder Fraga^{a,b,1}; Joaquim G. Pinto^b; Francesco Viola^c; João A. Santos^a

3

4 ^a*Centre for the Research and Technology of Agro-Environmental and Biological Sciences*
5 *(CITAB), Universidade de Trás-os-Montes e Alto Douro (UTAD), Vila Real, Portugal*

6 ^b*Institute for Meteorology and Climate Research (IMK-TRO), Karlsruhe Institute of*
7 *Technology (KIT), Karlsruhe, Germany*

8 ^c*Department of Civil Environmental and Architectural Engineering, Università degli Studi di*
9 *Cagliari, Cagliari, Italy*

10

11 **Short title:** European olive trees under climate change scenarios

12

13

Revision 1 submitted to:

14

International Journal of Climatology

15

¹The corresponding author: Helder Fraga, E-mail: hfraga@utad.pt, Tel: +351259350000

16 **Abstract**

17 The olive tree is one of the most important crops in the Mediterranean basin. Given the strong
18 climatic influence on olive trees, it becomes imperative to assess climate change impacts on
19 this crop. Herein, these impacts were innovatively assessed, based on an ensemble of state-of-
20 the-art climate models, future scenarios and dynamic crop models. The recent-past (1989–
21 2005) and future (2041–2070, RCP4.5 and RCP8.5) olive growing season length (GSL),
22 yield, growing season temperature (GST) and precipitation (GSP), potential (ETP) and actual
23 (ETA) evapotranspiration, water demand (WD) and water productivity (WP), were assessed
24 over southern Europe. Crop models were fed with an ensemble of EURO-CORDEX regional
25 climate model data, along with soil and terrain data. For the recent-past, important differences
26 between western and eastern olive growing areas are found. GSL presents a strong latitudinal
27 gradient, with higher/lower values at lower/higher latitudes. Yields are lower in inner south
28 Iberia and higher in Italy and Greece, which is corroborated by historical data. Southern Iberia
29 shows higher GST and lower GSP, which contributes to a higher ETP, lower ETA and
30 consequently stronger WD. Regarding WP, the recent-past values shows similar ranges across
31 Europe. Future projections point to a general increase in GSL along with an increase in GST
32 up to 3°C. GSP is projected to decrease in Western Europe, leading to enhanced WD and
33 consequently a yield decrease (down to -45%). Over eastern European, GSP is projected to
34 slightly increase, leading to lower WD and to a small yield increase (up to +15%). WP will
35 remain mostly unchanged. We conclude that climate change may negatively impact the
36 viability of olive orchards in southern Iberia and some parts of Italy. Thus, adequate and
37 timely planning of suitable adaptation measures are needed to ensure the sustainability of the
38 olive sector.

39 **Keywords:** Olive yields; Europe; climate change; Euro-Cordex; Representative
40 Concentration Pathways

42 1. Introduction

43 The olive tree (*Olea europaea* L.) is one of the oldest permanent crops grown in the
44 Mediterranean basin (Vossen, 2007). This perennial and evergreen tree has a strong socio-
45 economic importance for many southern European countries, which encompass 80% of the
46 worldwide olive tree area (EC, 2012) (Fig. 1) and produce roughly 95% of the world olive oil
47 supply. Olive production is concentrated in the Mediterranean-type climatic regions of
48 southern Europe, particularly Spain (53%), Italy (24%), Greece (15%) and Portugal (7%) ,
49 amongst others (EC, 2012). Since olive oil is traditionally exported worldwide, this crop
50 became one of the foundations for the economic development in agrarian regions in these
51 countries (IOC, 2018).

52 Traditional olive orchards in the Mediterranean basin present very specific climatic
53 requirements, required to attain high production levels and quality attributes (Vossen, 2007).
54 This crop is considered one of the most suitable and best adapted species to the
55 Mediterranean-type climate (Moriondo *et al.*, 2015, Orlandi *et al.*, 2012). In fact, the location
56 of olive orchards in this specific region of the globe is primarily explained by climatic factors.
57 While temperatures below -5 °C damage olive branches and significantly limit its poleward
58 expansion, the lack of cold temperatures - necessary to ensure a proper flowering - limit its
59 equatorward distribution (Moriondo *et al.*, 2015). Olives are also very drought-tolerant, as the
60 lower limit for annual precipitation is around 350 mm (Ponti *et al.*, 2014). As such, the olive
61 tree is usually grown under rain-fed conditions (Gomez-Rico *et al.*, 2007). All these aspects
62 make the olive tree particular suitable for the Mediterranean-type climate (Moriondo *et al.*,
63 2015), which is characterized by warm dry summers and rainy winters. However, soil fertility
64 and soil water holding capacity may also play an important role for olive tree development.

65 The Mediterranean basin is considered a climate change “hotspot” (Giorgi, 2006), since future
66 projections point to considerable warming trends and an increase of consecutive dry days for
67 this area (IPCC, 2012), leading to an overall increase in aridity. In this context, climate
68 change may become particularly challenging for olive growers (Moriondo *et al.*, 2015).
69 Recent studies applied to olive trees have shown that this crop can be strongly affected by
70 climate change (Orlandi *et al.*, 2005, Osborne *et al.*, 2000, Ponti *et al.*, 2014) particularly
71 under the Mediterranean type-climates (Galán *et al.*, 2005, Orlandi *et al.*, 2010). For instance,
72 rising temperatures may have strong impacts on this crop, advancing phenological timings,
73 particularly flowering (Avolio *et al.*, 2012, Galán *et al.*, 2005, Orlandi *et al.*, 2010, Osborne *et*
74 *al.*, 2001). Fraga *et al.* (2019) points to a strong change in thermal conditions for olive trees in
75 Europe until the end of this century. Other studies suggest a gradual poleward shift of current
76 olive cultivation areas in the upcoming decades, due to increased suitability in higher latitudes
77 (Moriondo *et al.*, 2013, Tanasijevic *et al.*, 2014). In spite of these efforts, there is a strong
78 need to improve our knowledge on how future climate may affect olive yields. As an
79 example, Ponti *et al.* (2014), using a single future climate scenario (A1B) and a single climate
80 model, projected high economic losses for small olive farms in Italy and Greece. Still, there is
81 a need to perform comprehensive assessments based on multi-model multi-scenario
82 ensembles in order to derive robust yield estimates and provide a measure of its uncertainty
83 under future climate conditions (Deser *et al.*, 2012).

84 Crop models are gradually becoming reliable tools to support decision making within the
85 agrarian sector (Challinor & Wheeler, 2008, Paz *et al.*, 2007, Semenov & Doblaz-Reyes,
86 2007). Crop models can be either statistical/empirical or dynamical/process-based in their
87 nature. While statistical models try to establish relationships between e.g. historical yields and
88 climate data, dynamic models inherently simulate plant growth and development by
89 integrating varietal information, soil characteristics, weather data and management practices

90 (Moriondo *et al.*, 2015). Despite being applied to a large array of crops worldwide (e.g.
91 wheat, maize, rice), crop models are still not widely used for olive trees. Still, some statistical
92 models do exist, which relate growing season temperatures, particularly during spring, with
93 phenological timings and yields (Aguilera *et al.*, 2015, Garcia-Mozo *et al.*, 2008, Moriondo *et*
94 *al.*, 2001, Orlandi *et al.*, 2012, Oteros *et al.*, 2014, Quiroga & Iglesias, 2009). Regarding
95 dynamical models, some models are devoted to access phenological stages of olive tree
96 growth and development (Cesaraccio *et al.*, 2004, De Melo-Abreu *et al.*, 2004, Moriondo *et*
97 *al.*, 2019), while others are aimed to predict biomass growth (Maselli *et al.*, 2012, Villaobos
98 *et al.*, 2006, Viola *et al.*, 2012). Given their large complexity, dynamic models usually tend to
99 be preferable to statistical approaches, as they simulate plant physiology and its relationships
100 with the surrounding environment. Furthermore, dynamical models are continuously updated
101 with new scientific knowledge. These dynamical crop models can thus lead to reliable and
102 robust future projections of yield, growing season length and stress indicators over a wide
103 region when coupled with high resolution climate model simulations, consistent soil and plant
104 data.

105 The present study aims to develop and analyse climate change projections for the olive sector
106 in the Mediterranean basin. As such, the objectives of this study are three-fold: 1) to couple a
107 dynamic crop model with high resolution climatic simulations for current climates and for
108 future climate change scenarios; 2) to develop climate change projections for olive yield,
109 growing season and stress conditions in the most important olive producing regions in the
110 Mediterranean basin; and 3) to discuss the impacts of climate change on the European olive
111 sector and possible adaptation measures.

112

113 2. Material and Methods

114 2.1 Study area

115 In order to assess the distribution of olive orchards in southern Europe, the CORINE Land
116 Cover (CLC, v18.5.1), was used. This dataset is derived from satellite imagery and mapping
117 of land inventories, providing land usage classes over most of Europe. The olive orchard
118 polygons were extracted for subsequent processing. All computations in the present study
119 were performed only inside the current olive orchard land cover delimitations (**cf. Fig. 1**). A
120 more detailed analysis was also performed on some of the European top olive producing
121 regions, such as (from west-to-east): (1) Alentejo in Portugal; (2) Andalucía, (3) Extremadura
122 and (4) Castilla la Mancha in Spain; (5) Sardegna , (6) Sicily and (7) Puglia in Italy; and (8)
123 Peloponnese in Greece (**Fig. 1**). For this purpose, the Nomenclature of Territorial Units for
124 Statistics - level 2 (NUTS-2) classification was used to delineate the regions. Other olive
125 growing regions were not considered due to limitations in the various datasets.

126

127 2.2 Crop Model description

128 To model olive yields, the dynamic crop model developed by Viola *et al.* (2012) was used
129 (henceforth yield-model). This is a water-driven crop model that “links olive yield to climate
130 and soil moisture dynamics using an ecohydrological approach” (Viola *et al.*, 2012). In a
131 recent review of current dynamic crop models applied to olive trees, Moriondo *et al.* (2015)
132 described this model underlining the keys aspects. The leaf area index influences the light
133 interception model. Dry matter formation is governed by the photosynthesis and respiration
134 models. The photosynthesis model takes the atmospheric CO₂ levels into account, while the
135 transpiration model follows the implementation by Villalobos *et al.* (2000). The conversion of
136 biomass into final yield is influenced by water stress. Indeed, dry matter partitioning and

137 potential biomass are limited by water availability in the soil, which in turn is governed by
138 rainfall inputs and vegetation withdrawal. The latter, without soil moisture limitations is
139 modelled with the Penman-Monteith Big Leaf model, which explicitly takes into account the
140 effect of CO₂ concentration in the photosynthesis model. All simulations herein were
141 performed continuously without any re-initialization in order to examine certain carry-over
142 effects on the final yields, such as the stress duration and intensity. Other effects, such as
143 alternate bearing or changes in partition coefficients, are not considered. For additional
144 information regarding this model please see Viola *et al.* (2012).

145 This model runs on a daily time-step, simulating crop development from the start until the end
146 of the growing season and requires a large number of parameters describing local conditions,
147 such as soil profile characteristics (e.g. soil hydraulic conductivity and soil porosity),
148 technical parameters (e.g. leaf area index, crop ground cover fraction, growing season start
149 and end) and weather daily data (precipitation, maximum and minimum temperatures,
150 radiation, relative humidity, wind speed and CO₂). All these parameters were used as model
151 input and are described in the subsequent sections.

152 In order to access the olive tree growing season (required by the yield-model), the model
153 developed by Orlandi *et al.* (2013) was used (henceforth season-model). This is a very simple
154 regional model that provides the annual start and end of the vegetative cycle (leaf
155 development start to fruit coloration) based on a bioclimatic “growing season index” of olive
156 trees (Orlandi *et al.*, 2013). This index is derived only from climatic data and was properly
157 validated for the Mediterranean olive tree areas (Orlandi *et al.*, 2013). Both models (season-
158 model and yield-model) were therefore coupled.

159

160 *2.3 Climate data*

161 The required daily meteorological variables by the two crop models are: maximum air
162 temperature ($^{\circ}\text{C}$), minimum air temperature ($^{\circ}\text{C}$), solar radiation ($\text{W}\cdot\text{m}^{-2}$), total precipitation
163 (Prec; mm), wind speed ($\text{m}\cdot\text{s}^{-1}$), relative humidity (%) and CO_2 levels (ppmv). All these
164 variables were obtained from EURO-CORDEX datasets (Jacob *et al.*, 2014), an ensemble of
165 regional climate model simulations at a ~ 12.5 km spatial resolution covering the southern
166 European sector. For the recent-past period (1989-2005), we consider four regional climate
167 models (RCM, **Table 1**) driven with ERA-Interim reanalysis (Dee *et al.*, 2011) as boundary
168 conditions (EURO-CORDEX evaluation runs). 1989-2005 was considered since it is the
169 overlapping time period available for all the climate models for the recent-past. This dataset
170 represents real-world climate over the selected period. Within the EURO-CORDEX project
171 framework, the RCMs were also forced by four global climate models (GCM, **Table 1**) for
172 1989-2005 (historical runs) and for 2041-2070 following the RCP4.5 and RCP8.5 scenarios.
173 In RCP4.5, CO_2 emissions are projected to increase until the mid-21st century, decreasing
174 afterwards (IPCC, 2012). In contrast, in RCP8.5, the CO_2 emissions continue to rise until the
175 end of the 21st century. The CO_2 values correspond to 497 and 598 ppm (on average for
176 2041-2070), for RCP4.5 and RCP8.5, respectively.

177 The daily variables produced by the RCM-GCM chains were first bias-corrected for 1989-
178 2005 using the evaluation runs as a reference and following the “Empirical Quantile
179 Mapping” methodology (Cofiño *et al.*, 2017). This correction was subsequently applied to the
180 future period (2041-2070), thus obtaining future bias corrected data. This methodology was
181 previously carried out by several studies, e.g. Fraga *et al.* (2019). Lastly, the bias-corrected
182 gridded climatic variables were then used as input for the crop models.

183

184 *2.3 Soil and plant data*

185 Each grid-box in the climatic datasets was treated as an independent site in the crop models.
186 Other required variables were defined based on the location of these grid-boxes, such as soil
187 and terrain characteristics. Soil data was obtained from the Harmonized World Soil Database
188 (HWSD; FAO/IIASA/ISRIC/ISSCAS/JRC, 2012). Soil properties from the HWSD were
189 extracted based on the predominant soil type inside each grid-box (**Table 2**). Some soil
190 parameters were estimated using the pedotransfer functions also described in **Table 2**. For a
191 large-scale comprehensive modelling approach throughout southern Europe, some
192 assumptions were made concerning grown varieties and cultural practices. Hence, plant data
193 was set as standard for all grid-boxes, following Viola *et al.* (2012): leaf area index ($1.4 \text{ m}^2 \cdot \text{m}^{-2}$);
194 root depth (100 cm) and canopy cover fraction (0.4).

195

196 *2.4 Modelling outputs*

197 The current study focuses only on the area currently covered by olive trees, which is mostly
198 confined to some regions in southern Europe (**Fig. 1**). Therefore, both the yield-model and the
199 season-model were run for all grid-boxes within these delimitations, separately for each
200 climate model and each year. While crop model runs were performed for each climate model
201 separately, the outcomes of these runs were averaged for all climate models (ensemble means)
202 in order to obtain more robust future projections. The annual outputs collected for the recent-
203 past and for each future scenario were: growing season start (GSS, calendar day), growing
204 season end (GSE, calendar day), growing season length ($\text{GSL} = \text{GSE} - \text{GSS}$ in number of
205 days), yield ($\text{kg} \cdot \text{ha}^{-1}$), growing season potential evapotranspiration (ETP, mm) and growing
206 season actual evapotranspiration (ETA, mm). Other two important water use related metrics
207 that greatly influence olive yields were also computed: the growing season water deficit (WD,
208 mm), which corresponds to ETP minus ETA (Moriondo *et al.*, 2013), and the growing season

209 water productivity (WP; $\text{kg}\cdot\text{ha}^{-1}\cdot\text{mm}$), i.e. yield divided by ETA (Perry, 2011). Additionally,
210 the growing season mean temperature (GST) and growing season precipitation (GSP) were
211 also computed. Lastly, the annual outcomes were averaged for each time period (1989–2005
212 and 2041–2070) and mapped throughout the southern European sector. Statistically
213 significant differences between the future and the recent-past were also assessed and mapped
214 at a 99% confidence level, using the two-sample *Student's t-test*.

215 Both crop models have been previously validated. Regarding the season-model, Orlandi *et al.*
216 (2013) showed a strong relationship between GSS (GSE) and leaf development start (fruit
217 coloration) (root-mean-squared errors of 1.73 or 0.58 days, respectively), over olive regions in
218 Italy, Spain and Tunisia. For the yield-model, Viola *et al.* (2012) successfully validated the
219 model for olive orchard site in Italy. Nonetheless, we perform a comparison between the
220 modelled yields and the national olive yield statistics from the Food and Agriculture
221 Organization of the United Nations (FAO; <http://faostat.fao.org/>) (**Fig. 1**). Additionally, data
222 from the EUROSTAT regional dataset was also collected, though a comparison was not
223 possible due to important data gaps found in this dataset, both spatially and temporally. This
224 data corresponds to a large number of varieties (mixed varieties) and years, which does not
225 exactly correspond to the historical time period used herein. Still, this validation effort is
226 useful to assess whether the yield-model is able to capture the magnitude and heterogeneity of
227 yield values in Europe.

228

229 **3. Results**

230 *3.1 Recent-past assessment*

231 The GSL for the recent-past, computed by the season-model, is shown in **Figure 2a**. Overall,
232 the olive tree GSL ranges from 200 days in the cooler regions of northern Italy and southern
233 France, to 220-230 days in Iberia, Greece, Albania and southern Italy, reaching a maximum of
234 250 in southern Iberia. A latitudinal gradient is clearly visible in the GSL patterns, where the
235 northern (southern) regions show lower (higher) number of days in the growing season. This
236 indicates that the olive tree growing season is typically longer for western Europe.

237 Regarding yields (**Fig. 2b**), the simulations show higher values in Italy and some areas of
238 Albania and Greece (>2000 kg/ha) and lower values in southeastern Iberia (~1000 kg/ha). The
239 magnitude of the simulated values is in agreement with the regional statistical dataset (**Fig. 1**),
240 and the model is also able to resolve longitudinal yield differences that are visible in the
241 statistical dataset, e.g., the higher yields in Italy and Greece compared to Iberia. Still, some
242 discrepancies are found between the simulated and the statistical dataset. Overall, the model
243 simulates slightly higher values than those found in the statistical dataset (**Fig. 1**).

244 GST for the recent-past (**Fig. 2c**) ranges from 12 °C at higher elevation and cooler areas to 24
245 °C in inner Iberia and some regions in southeastern Italy and in Greece. The cooler regions
246 include northern Portugal, northern Italy and in the (southern) French olive growing regions.

247 Regarding GSP (**Fig. 2d**), the map presents very homogeneous patterns, with most of the
248 olive productive regions showing values from 200 to 300 mm, with the exception of areas in
249 central/northern Italy and in southern France, where precipitation amounts exceed 300 mm.

250 Water availability is an important factor affecting plant physiological activity, particularly in
251 arid and semi-arid regions, such as in the Mediterranean (Aissaoui *et al.*, 2016). For the
252 recent-past, the growing season ETP (**Fig. 2e**) shows higher values in southern Iberia, from
253 ~1000 mm to around 600 mm in northern Italy. However, most of the olive orchard areas in

254 southern Europe present ETP values from 800 to 1000 mm. In effect, ETP patterns are highly
255 correlated with the GST ($r = +0.8$), since temperature strongly influences this metric.

256 Regarding ETA (**Fig. 2f**), a metric that takes into account the amount of water that is
257 effectively used by the plant, this metric shows heterogeneous values across Europe. The
258 ETA ranges from 200 mm, in southeastern Iberia, to 500 mm, in some regions in inner Italy
259 and in coastal Croatia and Albania. Nonetheless, most of the olive orchards in Europe have
260 ETA values from 300 to 400 mm.

261 Given the difference between ETP and ETA, higher water deficits are found for the current
262 olive tree area (**Fig. 2g**), suggesting high water scarcity. During the growing season (**Fig. 2g**),
263 WD reaches values of ~ 750 mm in southern Iberia (in some areas even 900 mm), in Sicily
264 and in Sardegna. The lowest WD values are found in northern Italy, southern France and
265 some coastal areas of the Adriatic. Most of southern European olive orchards are thus
266 growing under relatively high water deficits. Regarding WP, this index displays relatively
267 homogeneous values throughout the olive growing areas (**Fig. 2h**). Values higher than 5
268 $\text{kg}\cdot\text{ha}^{-1}\cdot\text{mm}^{-1}$ are widespread, with the exception of some areas in inner Iberia, with values of
269 ca. $4 \text{ kg}\cdot\text{ha}^{-1}\cdot\text{mm}^{-1}$.

270

271 *3.2 Future climate projections*

272 The bias corrected projections from EURO-CORDEX (section 2.2.) are now considered to
273 estimate the impact of climate change to the olive orchards. Results point to an extension in
274 the length of the growing season under RCP4.5 (**Fig. 3a**) and RCP8.5 (**Fig. 4a**). In effect,
275 there is a clear increase of the GSL throughout Europe by up to 10 days, which hints at higher
276 temperatures throughout the growing season. The increase of the GSL ranges from 2 to 10
277 days, with the strongest increase occurring in south-eastern Spain and for RCP8.5. In some

278 parts of western Iberia, GSL values may remain largely unchanged, and this is the only area
279 where future projections for both scenarios are non-significant (NS).

280 Olive yields (**Fig. 3b and 4b**), are expected to decrease mostly in the Iberian Peninsula (-30%
281 to -45% in both scenarios) and some inner areas of Italy (down to -15%), whereas they are
282 expected to increase in other parts of Europe (up to +15%). It should be noted that the
283 increases in yields are comparatively small and tend to be NS. The outcomes for the two
284 future scenarios are in agreement, though a stronger climate change signal is expected under
285 RCP8.5 (**Fig 4b**). In order to assess the climate model uncertainty, i.e. differences between
286 the outputs from the four climate model pairs, the point-by-point normalized interquartile
287 ranges (NIQR) of the yield outputs from each model were computed. **Figure 5** shows that the
288 uncertainty is relatively low over all of southern Europe, with some small regions in Iberia
289 showing slightly higher uncertainties, mostly under RCP8.5. Hence, the climate change
290 projections provided by the ensemble of 4 RCM-GCM model chains may be considered as
291 robust.

292 Regarding GST under RCP4.5 and 8.5 (**Fig. 3c and 4c**, respectively), a clear warming of the
293 growing season is found throughout southern Europe, intensified under the severest scenario
294 (RCP8.5). In fact, GST is expected to increase by up to 2 or 3 °C (for RCP4.5 and RCP8.5,
295 respectively), leading to the increase in GSL. Larger changes are projected in inner Iberia, that
296 shows GST increases of 2.5°C with respect to the recent-past. Regarding future GSP (**Fig. 3d**
297 and **4d**, for RCP4.5 and 8.5, respectively), both scenarios depict important decreases in the
298 Iberian Peninsula, mainly under RCP8.5 (**Fig. 4d**). Conversely, increases up to 100 mm are
299 projected in GSP over the easternmost areas (Italy, Greece and Turkey), although for some of
300 these areas the results are NS.

301 ETP is expected to increase from 30 to 75 mm in RCP4.5 (**Fig. 3e**), and from 45 to 90 mm in
302 RCP8.5 (**Fig. 4e**). These results are in accordance with Tanasijevic *et al.* (2014), who
303 projected an olive ET increase of around 51(\pm 17) mm up to the middle of this century under
304 the A1B scenario. Southern Iberia is projected to have the strongest increase in this metric.
305 Contrarily to the ETP, ETA will decrease in most of the olive orchard area during the XXI
306 Century. Under RCP4.5 (**Fig. 3f**), these values will strongly decrease in southern Iberia (-75
307 mm), particularly in Portugal (-100 mm). Over southern France and northern Italy, there may
308 be a slight NS increase in ETA, as is the case of the increased GSP. Under RCP8.5 (**Fig. 4f**),
309 these impacts will be intensified, particularly in southern Iberia.

310 These projected changes (increase in ETP and decrease in ETA), higher water demands and
311 lower water availability, will enhance water stress for olive trees in the future. Under RCP4.5
312 (**Fig. 3g**), WD is expected to rise by 90 to 135 mm, particularly in southern Iberia. There are
313 some small regions where WD could decrease, especially along coastal areas in the Adriatic.
314 Under RCP8.5 (**Fig. 4g**), these changes are strengthened. Changes in WP are spatially
315 heterogeneous for both scenarios (**Fig. 3h and 4h**). WP tends to decrease in eastern southern
316 Iberia and in some regions of central Italy, decreasing elsewhere.

317

318 *3.3 Regional inter-annual variability in yields*

319 **Figure 6** depicts the box-plots representing simulated yields for all years and scenarios and
320 for each of the olive producing regions in Europe (from 1989 to 2005 for the recent-past and
321 from 2041 to 2070 for both RCPs). In terms of means and medians, all regions show lower
322 future yields (**Table 3**), with the exceptions of Puglia and Peloponnese, which show higher
323 yields for both future scenarios with respect to the present period. The strongest negative
324 impacts are found in Andalucía, Alentejo and Extremadura and for RCP8.5. Both scenarios

325 are in agreement in terms of climate change signal, while RCP8.5 provides the strongest
326 changes in magnitude, either positive or negative (**Table 3**).

327 Concerning the yield extremes (99th and 1st percentiles), future projections highlight stronger
328 variability in all regions. Regarding the interquartile ranges - IQR (75th percentile minus 25th
329 percentile), some regions show lower future inter-annual variability, such as Alentejo,
330 Andalucía, Extremadura and Castilla la Mancha, while others show higher future annual
331 variability, i.e. Sardegna, Sicily, Puglia and Peloponnese (**Fig. 6**). Thus, most regions are
332 expected to suffer negative impacts both in terms of yield losses and higher variability.

333

334 **4. Discussion and conclusions**

335 The present study focused on the application of crop models to quantify present (1989–2005)
336 and future (2041–2070) olive growing season climatic conditions over southern Europe,
337 including seasonal cycle length, yield, water demand and water productivity. Under recent
338 climatic conditions, the season-model shows a latitudinal gradient, i.e. the olive tree growing
339 season is longer/shorter at lower/higher latitudes. The yield-model shows lower yields in
340 western European olive growing areas, especially in inner Iberia, whereas higher yields are
341 found in the eastern areas, such as Italy and Greece. Regarding the GST, higher values are
342 found in inner Iberia, while GSP shows similar values throughout European olive orchards,
343 with the exception of western Italy. Regarding ETP and ETA, they show patterns very similar
344 to GST and GSP, respectively. This also underlies higher WD in inner Iberia. Regarding WP,
345 similar values are found throughout the orchard areas in Europe.

346 Although the simulated yields depict an agreement with statistical datasets and the model
347 provides a realistic magnitude of yield values, some model bias were identified. These can be
348 attributed to inherent differences between simulated and statistical datasets, such as the

349 different time periods and different spatial resolution (country average data vs. grid data).
350 Additionally, the large spatial extent of the target area required some assumptions in model
351 parameterizations, such as regional cultural practices and varieties. These assumptions, such
352 as setting a fixed LAI or planting density throughout European olive orchards, may increase
353 the bias of the final outcomes, especially when considering that high density irrigated
354 orchards have been introduced in many areas. It is important to recognize that the regional
355 yield differences are not only dependant on regional soil and climate conditions, but also on
356 technological advances, higher plant density and other key agricultural operations.
357 Nonetheless, such detailed information is not currently available for the large spatial extent,
358 needed for the model runs. In fact, the Mediterranean basin encompasses a wide range of
359 olive tree varieties, different cultivation systems and agronomic practices (Moriondo *et al.*,
360 2015, Ponti *et al.*, 2014). While these factors restrict the prediction of yields over such a vast
361 area, they allow a thorough climate change impact assessment, as they take into account only
362 the climate change signal. Nonetheless, the different spatial gradients in European olive
363 growing regions were skilfully modelled, such as the differences in yields between the
364 western (lower yields) and eastern (higher yields) olive growing regions in southern Europe.
365 Another important aspect limiting the model prediction accuracy is tied to the model
366 development state. At the moment, perennial crop models, and consequently olive tree
367 models, present various limitations, which restrict their accuracy and application. As an
368 example, the models used herein do not explicitly consider the anthesis state, which might be
369 of major interest for growers. In the future, advances in crop modelling techniques and
370 development may surpass these limitations and thus permit wider applications.

371 The crop model projections indicate that olive trees will be affected by considerable
372 challenges in the future decades. The projections point to a general increase in the length of
373 the potential growing season (GSL), due to the increase in temperatures. As the heat

374 accumulation is generally higher, physiological activity may occur earlier. Although the
375 overall higher temperatures in the growing season may have positive impacts, other factors,
376 such as extreme temperatures during the warmer part of the year, may offset this positive
377 effect. These impacts are also intensified by the already reported advancement in olive
378 flowering (Avolio *et al.*, 2012, Orlandi *et al.*, 2012), which may bring additional threats to the
379 sector, such as the risk of pests and diseases (Ribeiro *et al.*, 2009). Our results also indicate
380 GST in southern Europe combined with lower/higher GSP in the western/eastern areas,
381 leading to a higher WD in the western olive producing regions, which will ultimately impact
382 yields. Hence, there is a clear cause-effect relationship between the increases in GST, ETP
383 and WD, the decreases in GSP and ETA, and the projected yield decrease for the future. Our
384 results suggest that olive productivity in Southern Europe will probably decrease in the
385 western areas, particularly in the Iberian Peninsula. These results are in agreement with older
386 studies using the A1B scenario (Ponti *et al.*, 2014, Tanasijevic *et al.*, 2014). Conversely,
387 climate change will tend to benefit some olive-producing areas particularly in the eastern parts
388 of southern Europe. These outcomes are not in line with Tanasijevic *et al.* (2014), who
389 suggests a decrease in suitability future rainfed olive cultivation in Italy and Greece. It should
390 be noted that the mentioned study uses an older IPCC scenario and older model simulations
391 (previous assessment report) and the current study uses an ensemble of state-of-the-art climate
392 models and two future RCPs.

393 Herein we show for the first time future impacts on European olive productivity based on an
394 ensemble of state-of-the-art climate models, future scenarios and crop models. Given the
395 results shown in the current study, climate change may negatively impact the viability of
396 farms in southern Iberia and, consequently, increase the risk of abandonment of olive groves
397 (de Graaff *et al.*, 2010). To cope with the projected changes, an adequate and timely planning
398 of suitable adaptation measures needs to be adopted by the olive sector, particularly in Iberia.

399 One of the main adaptation measures to future drier climates in these areas is the
400 improvement of water use efficiency. Water scarcity and competition will be one of the main
401 problems in these areas in the future, and smart irrigation strategies should be planned and
402 implemented (Gomez-Rico *et al.*, 2007, Orlandi *et al.*, 2012, Tanasijevic *et al.*, 2014). These
403 practices are already being adopted, accompanied by the implementation of intensive
404 plantation systems instead of traditional olive groves. As an example, smart irrigation systems
405 are already being installed in many groves in southern Spain (Tanasijevic *et al.*, 2014). This
406 indicates a growing concern about the future sustainability of the sector, as well as an
407 increasing awareness of the potential threats. However, sufficient water supply should be
408 taken into account, as in these areas this important resource is scarce, particularly due to the
409 prolonged low water availability periods during summer and to strong water competition, by
410 other crops (e.g. horticulture), by hydropower generation and by human consumption (e.g.
411 domestic use and tourism). An additional/complementary adaptation measure to irrigation
412 would be to increase WP, by selecting more adapted olive tree varieties, with higher drought
413 and heat tolerance, thus requiring less water to obtain similar yield levels. Regarding WD, it
414 should be mentioned that olive trees adapt exceptionally well to the typically dry conditions
415 of Mediterranean-type climates, e.g. by capturing water from soils under the wilting point,
416 which may result in actual lower WD.

417 Other adaptation measures should also be envisioned, which may provide additional positive
418 gains under climate change. Moreover, the implications of using intensive vs. traditional
419 systems should be studied (Patumi *et al.*, 1999). Longer-term measures should also be
420 anticipated, such as the northward shift of olive tree cultivation and/or its displacement to
421 higher elevations in order to avoid areas with severe/extreme heat stress (Orlandi *et al.*, 2012).
422 One potentially beneficial aspect of climate change that should be considered is the increase
423 in CO₂ levels. Some studies have shown that increased CO₂ concentration may bring positive

424 physiological effects, namely on photosynthesis (Drake *et al.*, 1997). In fact, the yield-model
425 considers this effect in the photosynthesis sub-model, which takes into account the CO₂
426 concentration. Hence, the present study considers this effect to a certain extent, as higher CO₂
427 may mitigate some of the negative effects of climate change, particularly droughts.

428 The adoption of suitable adaptation measures should be explored in each olive orchard, taking
429 into account their specificities, as they might be required to warrant the future sustainability
430 of the olive sector. In fact, the sector's ability to adapt to climate change will determine the
431 magnitude of the projected impacts (Quiroga & Iglesias, 2009). The current study is a first
432 approach using these crop models at such a large-scale level (Europe). It is thereby necessary
433 to continue evaluating and improving these tools so as to attain more accurate information
434 regarding climate change impacts on olive trees, as well as to develop effective and
435 sustainable adaptation measures to cope with climate change.

436

437 **Acknowledgements**

438 This work was funded by European Investment Funds (FEDER/COMPETE/POCI), POCI-01-
439 0145-FEDER-006958, and by the Portuguese Foundation for Science and Technology (FCT),
440 UID/AGR/04033/2013. The postdoctoral fellowship (SFRH/BPD/119461/2016) awarded to
441 the first author is appreciated. This work was partially funded by the FCT contract
442 CEECIND/00447/2017. JGP thanks the AXA Research Fund for support.

443

444 **Declaration on conflict of interest**

445 The authors declare no conflict of interest.

446 **References**

- 447 Aguilera F, Dhiab AB, Msallem M *et al.* (2015) Airborne-pollen maps for olive-growing
448 areas throughout the Mediterranean region: spatio-temporal interpretation.
449 *Aerobiologia*, 31, 421-434, <https://doi.org/10.1007/s10453-015-9375-5>.
- 450 Aissaoui F, Chehab H, Bader B *et al.* (2016) Early water stress detection on olive trees (*Olea*
451 *europaea* L. cvs 'chemlali' and 'Chetoui') using the leaf patch clamp pressure probe.
452 *Computers and Electronics in Agriculture*, 131, 20-28,
453 <https://doi.org/10.1016/j.compag.2016.11.007>.
- 454 Avolio E, Orlandi F, Bellecci C, Fornaciari M, Federico S (2012) Assessment of the impact of
455 climate change on the olive flowering in Calabria (southern Italy). *Theoretical and*
456 *Applied Climatology*, 107, 531-540, <https://doi.org/10.1007/s00704-011-0500-2>.
- 457 Cesaraccio C, Spano D, Snyder RL, Duce P (2004) Chilling and forcing model to predict bud-
458 burst of crop and forest species. *Agricultural and Forest Meteorology*, 126, 1-13,
459 <https://doi.org/10.1016/j.agrformet.2004.03.002>.
- 460 Challinor AJ, Wheeler TR (2008) Crop yield reduction in the tropics under climate change:
461 Processes and uncertainties. *Agricultural and Forest Meteorology*, 148, 343-356,
462 <https://doi.org/10.1016/j.agrformet.2007.09.015>.
- 463 Cofiño AS, Bedia J, Iturbide M *et al.* (2017) The ECOMS User Data Gateway: Towards
464 seasonal forecast data provision and research reproducibility in the era of Climate
465 Services. *Climate Services*, <https://doi.org/10.1016/j.cliser.2017.07.001>.
- 466 De Graaff J, Duarte F, Fleskens L, De Figueiredo T (2010) The future of olive groves on
467 sloping land and ex-ante assessment of cross compliance for erosion control. *Land*
468 *Use Policy*, 27, 33-41, <https://doi.org/10.1016/j.landusepol.2008.02.006>.
- 469 De Melo-Abreu JP, Barranco D, Cordeiro AM, Tous J, Rogado BM, Villalobos FJ (2004)
470 Modelling olive flowering date using chilling for dormancy release and thermal time.
471 *Agricultural and Forest Meteorology*, 125, 117-127,
472 <https://doi.org/10.1016/j.agrformet.2004.02.009>.
- 473 Dee DP, Uppala SM, Simmons AJ *et al.* (2011) The ERA-Interim reanalysis: configuration
474 and performance of the data assimilation system. *Quarterly Journal of the Royal*
475 *Meteorological Society*, 137, 553-597, <https://doi.org/10.1002/qj.828>.
- 476 Deser C, Phillips A, Bourdette V, Teng HY (2012) Uncertainty in climate change projections:
477 the role of internal variability. *Climate Dynamics*, 38, 527-546,
478 <https://doi.org/10.1007/s00382-010-0977-x>.

- 479 Drake BG, Gonzalezmeier MA, Long SP (1997) More efficient plants: A consequence of
480 rising atmospheric CO₂? Annual Review of Plant Physiology and Plant Molecular
481 Biology, 48, 609-639.
- 482 Ec (2012) Economic analysis of the olive sector. pp 10.
- 483 Fao/Iiasa/Isric/Iscas/Jrc (2012) Harmonized World Soil Database (version 1.2). FAO, Rome,
484 Italy and IIASA, Laxenburg, Austria.
- 485 Fraga H, Pinto JG, Santos JA (2019) Climate change projections for chilling and heat forcing
486 conditions in European vineyards and olive orchards: a multi-model assessment.
487 Climatic Change, 152, 179-193, <https://doi.org/10.1007/s10584-018-2337-5>.
- 488 Galán C, García-Mozo H, Vázquez L, Ruiz L, De La Guardia CD, Trigo MM (2005) Heat
489 requirement for the onset of the *Olea europaea* L. pollen season in several sites in
490 Andalusia and the effect of the expected future climate change. International Journal
491 of Biometeorology, 49, 184-188, <https://doi.org/10.1007/s00484-004-0223-5>.
- 492 Garcia-Mozo H, Orlandi F, Galan C *et al.* (2008) Olive flowering phenology variation
493 between different cultivars in Spain and Italy: modeling analysis. Theoretical and
494 Applied Climatology, 95, 385, <https://doi.org/10.1007/s00704-008-0016-6>.
- 495 Giorgi F (2006) Climate change hot-spots. Geophysical Research Letters, 33,
496 <https://doi.org/10.1029/2006gl025734>.
- 497 Gomez-Rico A, Salvador MD, Moriana A, Perez D, Olmedilla N, Ribas F, Fregapane G
498 (2007) Influence of different irrigation strategies in a traditional Cornicabra cv. olive
499 orchard on virgin olive oil composition and quality. Food Chemistry, 100, 568-578,
500 <https://doi.org/10.1016/j.foodchem.2005.09.075>.
- 501 Ioc (2018) International Olive Council statistical series. <http://www.internationaloliveoil.org>.
- 502 Ipc (2012) Managing the Risks of Extreme Events and Disasters to Advance Climate Change
503 Adaptation. A Special Report of Working Groups I and II of the Intergovernmental
504 Panel on Climate Change [Field, C.B., V. Barros, T.F. Stocker, D. Qin, D.J. Dokken,
505 K.L. Ebi, M.D. Mastrandrea, K.J. Mach, G.-K. Plattner, S.K. Allen, M. Tignor, and
506 P.M. Midgley (eds.)]. Cambridge University Press, Cambridge, UK, and New York,
507 NY, USA, 582 pp.
- 508 Jacob D, Petersen J, Eggert B *et al.* (2014) EURO-CORDEX: new high-resolution climate
509 change projections for European impact research. Regional Environmental Change,
510 14, 563-578, <https://doi.org/10.1007/s10113-013-0499-2>.

- 511 Maselli F, Chiesi M, Brilli L, Moriondo M (2012) Simulation of olive fruit yield in Tuscany
512 through the integration of remote sensing and ground data. *Ecological Modelling*, 244,
513 1-12, <https://doi.org/10.1016/j.ecolmodel.2012.06.028>.
- 514 Moriondo M, Ferrise R, Trombi G, Brilli L, Dibari C, Bindi M (2015) Modelling olive trees
515 and grapevines in a changing climate. *Environmental Modelling & Software*, 72, 387-
516 401, <https://doi.org/10.1016/j.envsoft.2014.12.016>.
- 517 Moriondo M, Leolini L, Brilli L *et al.* (2019) A simple model simulating development and
518 growth of an olive grove. *European Journal of Agronomy*, 105, 129-145,
519 <https://doi.org/10.1016/j.eja.2019.02.002>.
- 520 Moriondo M, Orlandini S, Nunttiis PD, Mandrioli P (2001) Effect of agrometeorological
521 parameters on the phenology of pollen emission and production of olive trees (*Olea*
522 *europaea* L.). *Aerobiologia*, 17, 225-232, <https://doi.org/10.1023/A:1011893411266>.
- 523 Moriondo M, Trombi G, Ferrise R *et al.* (2013) Olive trees as bio-indicators of climate
524 evolution in the Mediterranean Basin. *Global Ecology and Biogeography*, 22, 818-
525 833, <https://doi.org/10.1111/geb.12061>.
- 526 Orlandi F, Avolio E, Bonofiglio T, Federico S, Romano B, Fornaciari M (2012) Potential
527 shifts in olive flowering according to climate variations in Southern Italy.
528 *Meteorological Applications*, 20, 497-503, <https://doi.org/10.1002/met.1318>.
- 529 Orlandi F, Garcia-Mozo H, Dhiab AB *et al.* (2013) Climatic indices in the interpretation of
530 the phenological phases of the olive in mediterranean areas during its biological cycle.
531 *Climatic Change*, 116, 263-284, <https://doi.org/10.1007/s10584-012-0474-9>.
- 532 Orlandi F, Garcia-Mozo H, Galán C *et al.* (2010) Olive flowering trends in a large
533 Mediterranean area (Italy and Spain). *International Journal of Biometeorology*, 54,
534 151-163, <https://doi.org/10.1007/s00484-009-0264-x>.
- 535 Orlandi F, Ruga L, Romano B, Fornaciari M (2005) Olive flowering as an indicator of local
536 climatic changes. *Theoretical and Applied Climatology*, 81, 169-176,
537 <https://doi.org/10.1007/s00704-004-0120-1>.
- 538 Osborne CP, Chuine I, Viner D, Woodward FI (2000) Olive phenology as a sensitive
539 indicator of future climatic warming in the Mediterranean. *Plant Cell and*
540 *Environment*, 23, 701-710, <https://doi.org/10.1046/j.1365-3040.2000.00584.x>.
- 541 Osborne CP, Chuine I, Viner D, Woodward FI (2001) Olive phenology as a sensitive
542 indicator of future climatic warming in the Mediterranean. *Plant, Cell & Environment*,
543 23, 701-710, <https://doi.org/10.1046/j.1365-3040.2000.00584.x>.

- 544 Oteros J, Orlandi F, García-Mozo H *et al.* (2014) Better prediction of Mediterranean olive
545 production using pollen-based models. *Agronomy for Sustainable Development*, 34,
546 685-694, <https://doi.org/10.1007/s13593-013-0198-x>.
- 547 Patumi M, D'andria R, Fontanazza G, Morelli G, Giorio P, Sorrentino G (1999) Yield and oil
548 quality of intensively trained trees of three cultivars of olive (*Olea europaea* L.) under
549 different irrigation regimes. *Journal of Horticultural Science & Biotechnology*, 74,
550 729-737.
- 551 Paz JO, Fraisse CW, Hatch LU *et al.* (2007) Development of an ENSO-based irrigation
552 decision support tool for peanut production in the southeastern US. *Computers and*
553 *Electronics in Agriculture*, 55, 28-35, <https://doi.org/10.1016/j.compag.2006.11.003>.
- 554 Perry C (2011) Accounting for water use: Terminology and implications for saving water and
555 increasing production. *Agricultural Water Management*, 98, 1840-1846,
556 <https://doi.org/10.1016/j.agwat.2010.10.002>.
- 557 Ponti L, Gutierrez AP, Ruti PM, Dell'aquila A (2014) Fine-scale ecological and economic
558 assessment of climate change on olive in the Mediterranean Basin reveals winners and
559 losers. *Proceedings of the National Academy of Sciences of the United States of*
560 *America*, 111, 5598-5603, <https://doi.org/10.1073/pnas.1314437111>.
- 561 Quiroga S, Iglesias A (2009) A comparison of the climate risks of cereal, citrus, grapevine
562 and olive production in Spain. *Agricultural Systems*, 101, 91-100,
563 <https://doi.org/10.1016/j.agsy.2009.03.006>.
- 564 Ribeiro H, Cunha M, Abreu I (2009) A bioclimatic model for forecasting olive yield. *Journal*
565 *of Agricultural Science*, 147, 647-656, <https://doi.org/10.1017/s0021859609990256>.
- 566 Saxton KE, Rawls WJ, Romberger JS, Papendick RI (1986) Estimating Generalized Soil-
567 water Characteristics from Texture. *Soil Science Society of America Journal*, 50,
568 1031-1036, <https://doi.org/10.2136/sssaj1986.03615995005000040039x>.
- 569 Semenov MA, Doblaz-Reyes FJ (2007) Utility of dynamical seasonal forecasts in predicting
570 crop yield. *Climate Research*, 34, 71-81, <https://doi.org/10.3354/Cr034071>.
- 571 Tanasijevic L, Todorovic M, Pereira LS, Pizzigalli C, Lionello P (2014) Impacts of climate
572 change on olive crop evapotranspiration and irrigation requirements in the
573 Mediterranean region. *Agricultural Water Management*, 144, 54-68,
574 <https://doi.org/10.1016/j.agwat.2014.05.019>.
- 575 Villalobos FJ, Orgaz F, Testi L, Fereres E (2000) Measurement and modeling of
576 evapotranspiration of olive (*Olea europaea* L.) orchards. *European Journal of*
577 *Agronomy*, 13, 155-163, [https://doi.org/10.1016/S1161-0301\(00\)00071-X](https://doi.org/10.1016/S1161-0301(00)00071-X).

- 578 Villaobos FJ, Testi L, Hidalgo J, Pastor M, Orgaz F (2006) Modelling potential growth and
579 yield of olive (*Olea europaea* L.) canopies. *European Journal of Agronomy*, 24, 296-
580 303, <https://doi.org/10.1016/j.eja.2005.10.008>.
- 581 Viola F, Noto LV, Cannarozzo M, La Loggia G, Porporato A (2012) Olive yield as a function
582 of soil moisture dynamics. *Ecohydrology*, 5, 99-107, <https://doi.org/10.1002/eco.208>.
- 583 Vossen P (2007) Olive oil: History, production, and characteristics of the world's classic oils.
584 *HortScience*, 42, 1093-1100.

585

586

Peer Review Only

587 **Table 1** – List of the regional climate models (RCM) and used boundary conditions from
588 global climate models (GCM) used in this study.

RCM	GCM
CLMcom-CCLM4-8-17	MPI-M-MPI-ESM-LR
IPSL-INERIS-WRF331F	IPSL-IPSL-CM5A-MR
KNMI-RACMO22E	ICHEC-EC-EARTH
SMHI-RCA4	CNRM-CERFACS-CNRM-CM5

589

Peer Review Only

590 **Table 2** - Soil and terrain parameters used in the crop model, along with the corresponding
 591 datasets used for their calculation and key references.

Parameter	Calculation
Clay content (%)	HWSD
Sand content (%)	HWSD
Silt content (%)	HWSD
Field capacity fraction ($\text{cm}^3 \cdot \text{cm}^{-3}$)	Estimated following Saxton <i>et al.</i> (1986)
Soil porosity ($\text{cm}^3 \cdot \text{cm}^{-3}$)	Estimated following Saxton <i>et al.</i> (1986)
hydraulic conductivity ($\text{cm} \cdot \text{day}^{-1}$)	Estimated following Saxton <i>et al.</i> (1986)

592

593 **Table 3** – Regional mean differences, in percentage, between future (2041–2070) RCP4.5/8.5
 594 and the present annual mean yields.

#	Region	RCP4.5	RCP8.5
1	Alentejo-PT	-17	-20
2	Andalucía-ES	-17	-21
3	Extremadura-ES	-15	-19
4	Castilla la Mancha-ES	-18	-19
5	Sardegna-IT	-8	-3
6	Sicily-IT	0	-8
7	Puglia-IT	5	7
8	Peloponnese-GR	4	3

595

596 **Figures**

597 **Fig. 1** – Olive orchard distribution in Europe following the CORINE land cover dataset. The
598 different color represent country yields according to FAO statistics. Additionally some of
599 Europe top olive producing regions are also represented following NUTS 2 level
600 delimitations.

601 **Fig. 2** – Patterns for the recent-past (1989-2005) for *a)* Growing season length (days), *b)* yield
602 ($\text{kg}\cdot\text{ha}^{-1}$), *c)* growing season mean temperature ($^{\circ}\text{C}$), *d)* Growing season precipitation sum
603 (mm), *e)* potential evapotranspiration in the growing season (mm), *f)* actual
604 evapotranspiration in the growing season (mm), *g)* water deficit (ETP minus ETA; mm) in
605 the growing season, *h)* Water productivity ($\text{kg}\cdot\text{ha}^{-1}\cdot\text{mm}$; yield divided by ETA) in the growing
606 season.

607 **Fig. 3** – Patterns for the differences between future RCP4.5 (2041-2070) and recent-past
608 (1989-2005) for the same variables as in Figure 2. Statistically significant (p -value < 0.01)
609 and non-significant differences are also plotted in grey shading.

610 **Fig. 4** – Same as Figure 3 but for RCP8.5.

611 **Fig. 5** – Model uncertainty represented by the yield normalized interquartile range of the 4
612 RCM-GCM model chains under a) RCP4.5 and b) RCP8.5.

613 **Fig. 6** – Box-plots representing the inter-annual variability in yields in the main Olive
614 producing regions in Europe, for the present (1989-2005), RCP4.5 (2041-2070) and RCP8.5
615 (2041-2070).

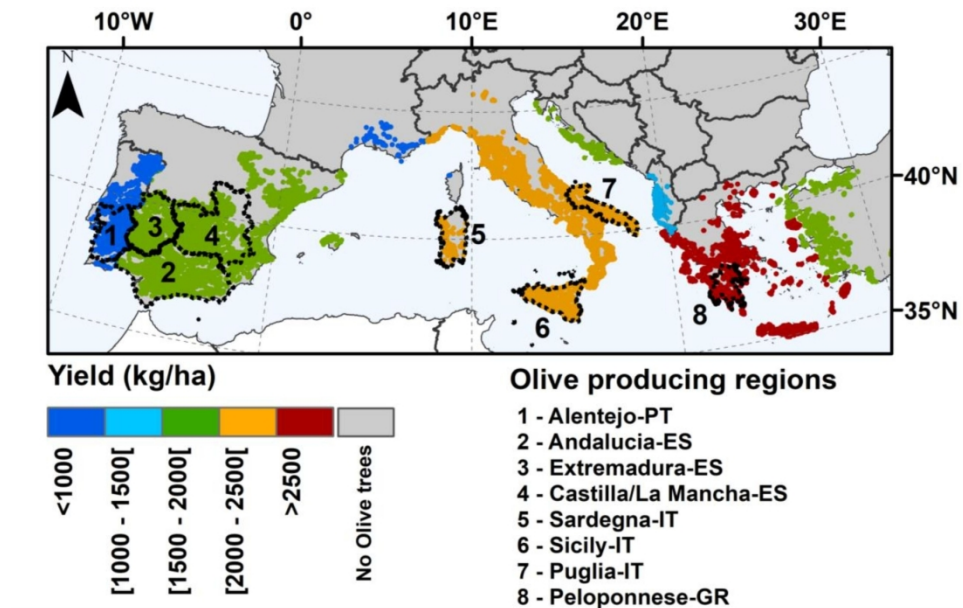


Figure 1: Olive orchard distribution in Europe following the CORINE land cover dataset. The different color represent country yields according to FAO statistics. Additionally some of Europe top olive producing regions are also represented following NUTS 2 level delimitations.

169x115mm (300 x 300 DPI)

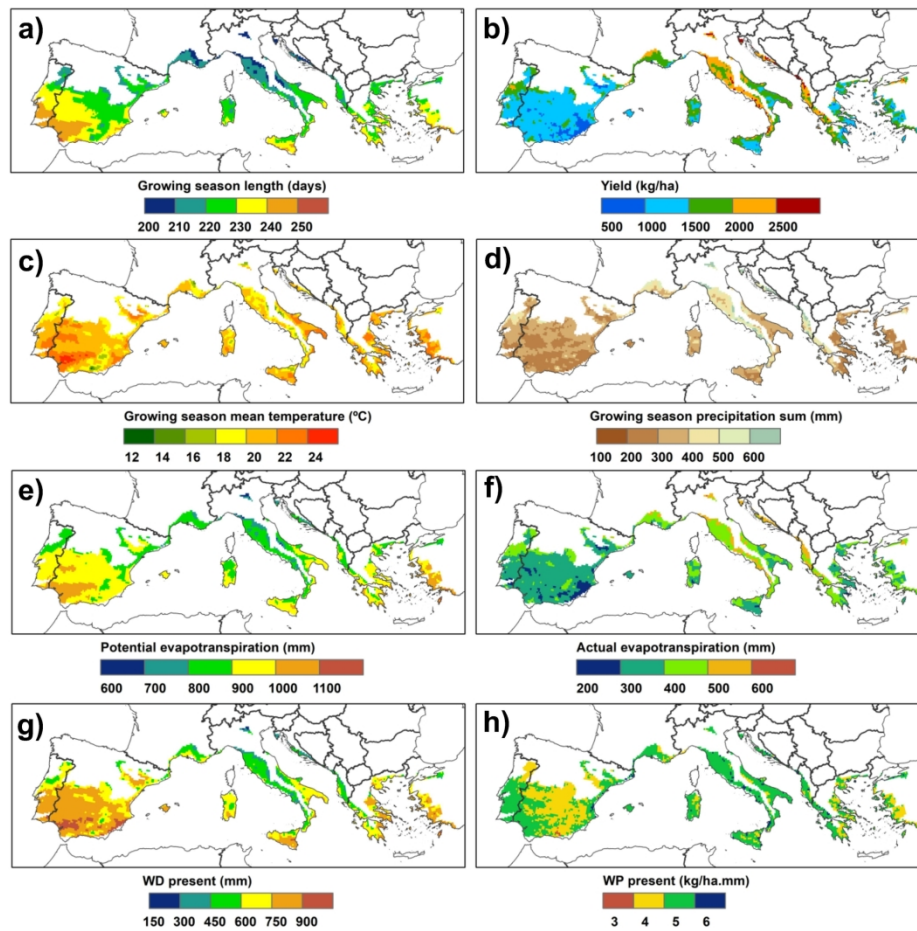


Figure 2: Patterns for the recent-past (1989-2005) for a) Growing season length (days), b) Potential yield (kg.ha⁻¹), c) growing season mean temperature (°C), d) Growing season precipitation sum (mm), e) potential evapotranspiration in the growing season (mm), f) actual evapotranspiration in the growing season (mm), g) water deficit (ETP minus ETA; mm) in the growing season, h) Water productivity (kg.ha⁻¹.mm; yield divided by ETA) in the growing season.

190x187mm (300 x 300 DPI)

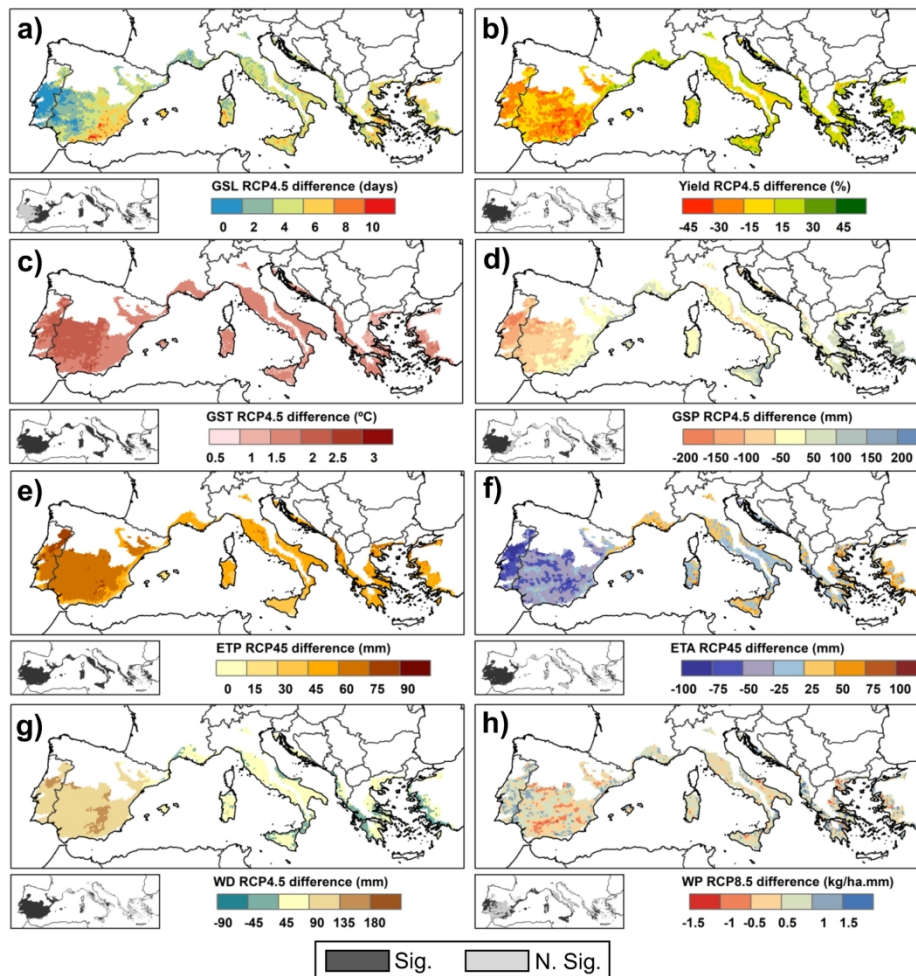


Figure 3: Patterns for the differences between future RCP4.5 (2041-2070) and recent-past (1989-2005) for the same variables as in Figure 2. Statistically significant (p -value < 0.01) and non-significant differences are also plotted in grey shading.

190x199mm (300 x 300 DPI)

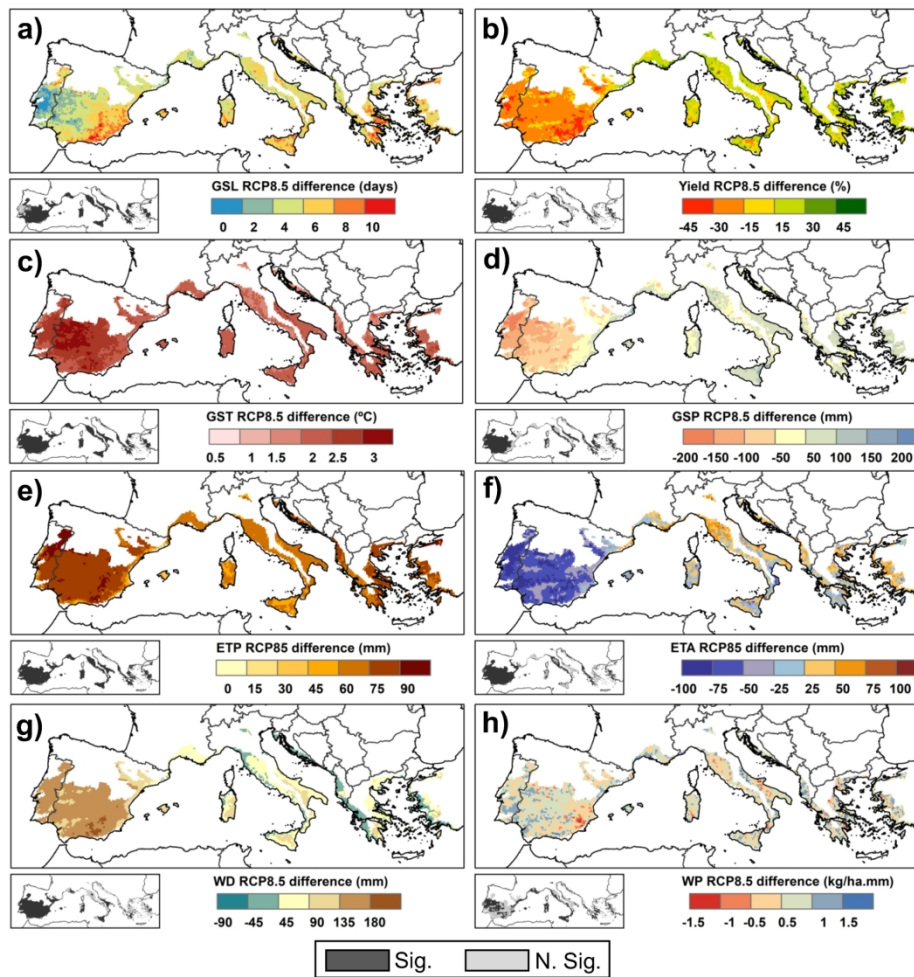


Figure 4: Same as Figure 3 but for RCP8.5.

190x197mm (300 x 300 DPI)

Model uncertainty (NIQR)

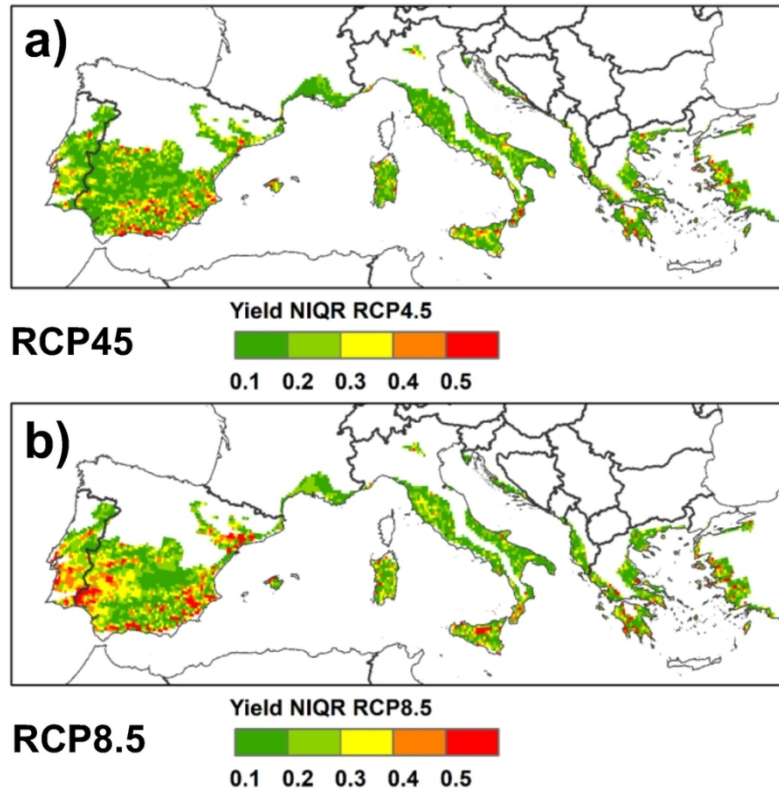


Figure 5: Model uncertainty represented by the yield normalized interquartile range of the 4 RCM-GCM model chains under a) RCP4.5 and b) RCP8.5.

110x103mm (300 x 300 DPI)

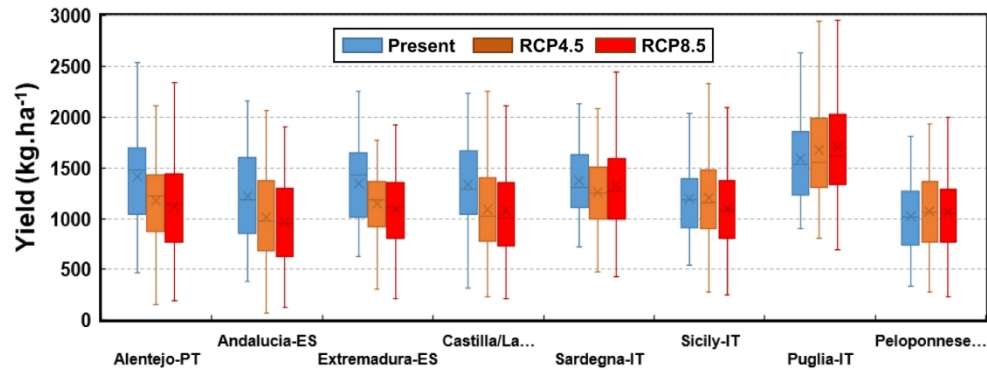
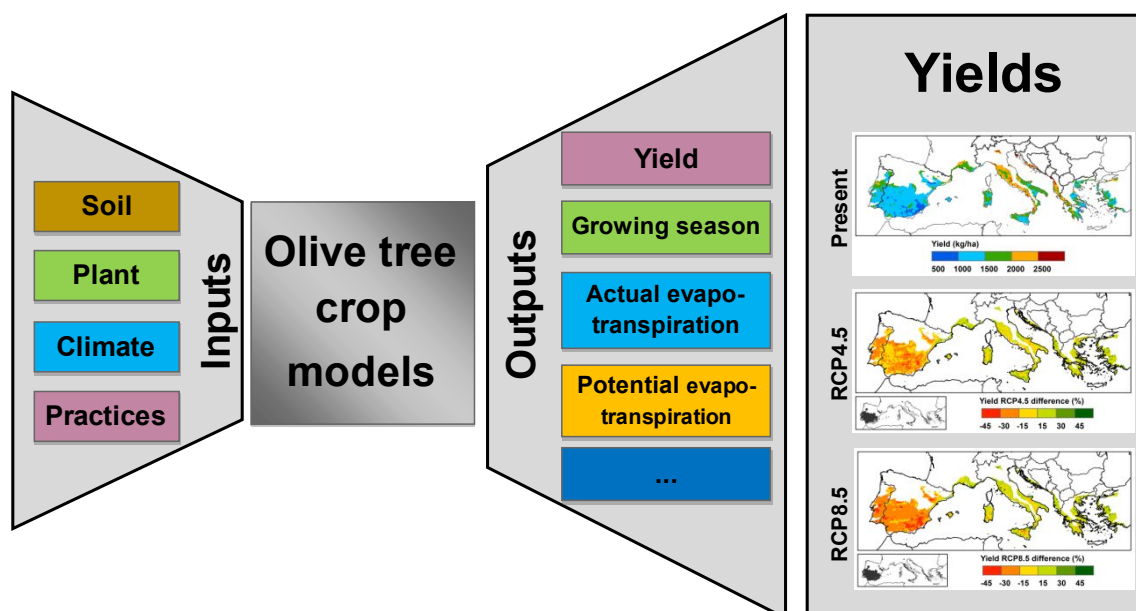


Figure 6: Box-plots representing the inter-annual variability in yields in the main Olive producing regions in Europe, for the present (1989-2005), RCP4.5 (2041-2070) and RCP8.5 (2041-2070).

190x73mm (300 x 300 DPI)

Climate change projections for olive yields in the Mediterranean Basin

Helder Fraga*; Joaquim G. Pinto; Francesco Viola; João A. Santos



Caption: Representation of the dynamical crop models used in the present study, along with the main inputs and outputs. Yield outputs of the recent-past and future (RCP4.5 and 8.5, mean of 4 RCM-RCM model-chain ensemble) are also shown. In some parts of Eastern Europe, future yields are projected to increase by 15%. Conversely, in the warmest and driest areas of Iberia, future yields may decrease to -45%. Adaptation measures should be adopted to counteract these negative impacts under climate change scenarios.